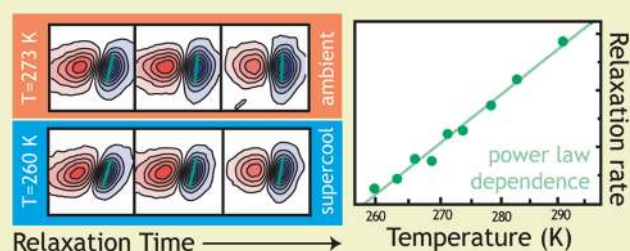


## Two-Dimensional Infrared Spectroscopy of Supercooled Water

Fivos Perakis and Peter Hamm\*

Physikalisch-Chemisches Institut, Universität Zürich, Winterthurerstrasse 190, CH-8057 Zürich, Switzerland

**ABSTRACT:** We present two-dimensional infrared (2D IR) spectra of the OD stretch vibration of isotope diluted water (HOD/H<sub>2</sub>O) from ambient conditions (293 K) down to the metastable supercooled regime (260 K). We observe that spectral diffusion slows down from 700 fs to 2.6 ps as we lower the temperature. A comparison between measurements performed at the magic angle with those at parallel polarization shows that the 2D IR line shape is affected by the frequency-dependent anisotropy decay in the case of parallel polarization, altering the extracted correlation decay. A fit within the framework of an Arrhenius law reveals an activation energy of  $E_a = 6.2 \pm 0.2$  kcal/mol and a pre-exponential factor of  $1/A = 0.02 \pm 0.01$  fs. Alternatively, a power law fit results in an exponent  $\gamma = 2.2$  and a singularity temperature  $T_s = 221$  K. We tentatively conclude that the power law provides the better physical picture to describe the dynamics of liquid water around the freezing point.



## INTRODUCTION

Liquid water's anomalies at ambient conditions, such as the compressibility minimum at 46 °C or the density maximum at 4 °C, are believed to be remnants of more pronounced low temperature anomalies. As the temperature is lowered, macroscopic properties of water, such as density, compressibility, thermal expansion coefficient, and heat capacity, seem to deviate from those of simple liquids.<sup>1</sup> The origin of these unusual properties lies in the fact that the H<sub>2</sub>O molecule acts both as a donor and acceptor,<sup>2</sup> leading to the formation of a random three-dimensional hydrogen bonding network which fluctuates on ultrafast time scales. In liquid water, depending on the temperature, this may give rise to different hydrogen bonding motifs, which at ambient conditions seem to coexist as structural and dynamic heterogeneities.<sup>3–5</sup> Going down to the supercooled regime, these heterogeneities appear to be more pronounced,<sup>6–8</sup> and it is hypothesized that they can be understood as the residual of two distinct liquid phases.<sup>9,10</sup>

One way to acquire information about this hydrogen bonding network is to monitor the changes of the OH (or OD) stretch frequency. The hydroxyl stretch is sensitive to the number and strength of the molecular hydrogen bonds. This leads to a distribution of frequencies originating from molecules at different local environments and results in the inhomogeneously broadened OH stretch band.<sup>11</sup> A measure sensitive to the dynamical changes of these local environments is the frequency fluctuation correlation function (FFCF),<sup>12,13</sup> a conditional probability that reveals the correlation loss of the system. In the case of water FFCF reveals the time scales of the hydrogen-bonding network rearrangements.

A number of theoretical and experimental spectroscopic studies have quantified this correlation decay for bulk water at ambient conditions (50 fs),<sup>14,15</sup> as well as for isotopic mixtures of

HOD/H<sub>2</sub>O (800 fs to 1.4 ps)<sup>16–18</sup> and HOD/D<sub>2</sub>O (900 fs to 1.2 ps).<sup>19,20</sup> From temperature-dependent simulations<sup>21,22</sup> and experimental studies of isotope-diluted water, ranging from ambient conditions<sup>23,24</sup> up to the supercritical regime,<sup>25</sup> it is understood that FFCF decay depends critically on temperature. Furthermore from time-resolved optical Kerr effect (HD-OKE) measurements in supercooled water it has been observed that water dynamics are characterized by a distribution of different time scales because of the presence of a variety of relaxing structures.<sup>26</sup>

Therefore, to investigate how the metastable limit can affect the hydrogen-bonding dynamics and quantify the change of the FFCF, we measure the spectral diffusion of the OD stretch vibration of HOD in H<sub>2</sub>O using two-dimensional infrared (2D IR) spectroscopy, for temperatures ranging from ambient conditions (293 K) down to the supercooled regime (260 K). The measurements are performed at the magic angle to decouple as much as possible the part of the correlation decay that is attributed to the hydrogen-bonding rearrangements, from the part which is due to frequency-dependent anisotropy decay.<sup>27,28</sup>

## EXPERIMENTAL METHODS

Ultrafast 800 nm pulses are generated by a commercial Ti:sapphire oscillator and chirped pulse amplifier of 1 mJ at a repetition rate of 1 kHz. A home-built optical parametric amplifier (OPA)<sup>29</sup> is used to generate 1.8  $\mu$ J tunable compressed mid-IR pulses of  $\approx 65$  fs duration (estimated by an interferometric autocorrelation measurement), centered at 2500 cm<sup>-1</sup>, with a bandwidth of

**Special Issue:** Shaul Mukamel Festschrift

**Received:** September 27, 2010

**Revised:** November 3, 2010

**Published:** November 29, 2010

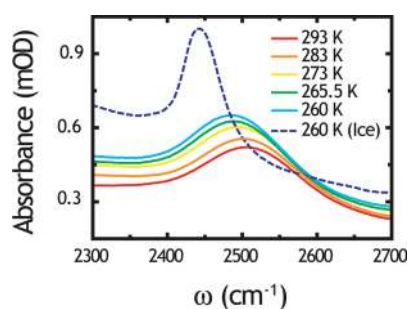


**Figure 1.** Temperature-dependent FTIR spectra of the OD stretch band of 5% HOD in H<sub>2</sub>O from 293 K down to 260 K. Solid lines: liquid and supercooled water; dashed line: ice.

250 cm<sup>-1</sup>. For the 2D measurements we used a Fourier transform 2D IR setup in pump-probe geometry.<sup>30,31</sup> The data acquisition is performed with a fast-scanning routine without phase ambiguity, described in detail elsewhere.<sup>31</sup> We perform measurements at the magic angle as well as at parallel polarization  $\langle ZZZZ \rangle$  geometry. Overall, we measured throughout the temperature range 293–260 K, for 25 population times between 50 fs and 3 ps. Purging with N<sub>2</sub> is necessary due to CO<sub>2</sub> absorption in this frequency range.

The sample consists of 2.5% D<sub>2</sub>O in triple-distilled and filtered H<sub>2</sub>O. A spacer of 6 μm is used, separating two CaF<sub>2</sub> windows of 2 mm thickness and scratch and dig quality 20/40. For the temperature control we use two Peltier coolers, the cold side of which is in contact with the windows, intermediated by a thin layer of thermally conductive paste. The warm side of the Peltiers is in contact with an ethanol bath which is circulated by a chiller set at 253 K. This allows higher precision for the Peltier temperature base ( $\pm 0.1$  K), providing the flexibility to immediately restore ambient conditions in the event of nucleation. The most decisive parameters for preventing nucleation turn out to be the use of small volume (0.2 μL), the assembly of the sample cell in a nitrogen purged glovebox (to reduce the presence of dust particles), and the use of new windows for each measurement, as well as preventing contact with the sample and the spacer, which tends to act as a source of nucleation.

## RESULTS

Figure 1 shows the Fourier transform infrared (FTIR) spectrum of the OD stretch of 5% HOD in H<sub>2</sub>O. Solid lines indicate liquid water ranging from 293 K down to 260 K, whereas dashed ones denote the ice spectrum at 260 K. Lowering the temperature, the OD stretch peak red shifts and narrows, and the absorbance increases, as a result of an overall strengthening of the hydrogen-bond network.<sup>21</sup>

A selection of purely absorptive 2D IR spectra of the OD stretch is shown in Figure 2. Spectra for different population times ( $t_2 = 50$  fs; 500 fs; 1, 2, and 3 ps) are depicted horizontally, whereas they are depicted vertically for different temperatures ( $T = 293, 273, 265.5,$  and 260 K). The blue lobe of the spectra is associated with ground state processes, that is, stimulated emission and bleaching of the 0–1 transition. Shifted to lower frequencies due to the anharmonic shape of the potential surface is the red lobe, associated with excited state absorption (1–2 transition).

The signal intensity decreases as a function of population time  $t_2$  due to vibrational relaxation (this effect is normalized out in Figure 2 to facilitate a better comparison of the 2D IR line shape,

which is discussed below). In Figure 3, we display this decay for the two extreme temperatures, where the signal is extracted as the change of the maximum value of the 2D IR spectra. Observe in Figure 3b that the change is very small throughout this temperature range (the relaxation changes from 1.25 to 1.35 ps), in agreement with other temperature-dependent studies of vibrational population relaxation.<sup>32</sup>

What is more important is the change of the 2D IR line shapes. For early population times, the spectra are more tilted along the diagonal, while later they are more rounded. This transformation carries information concerning the dynamics changes of the local environment. For small  $t_2$  there is little time for the molecules to change hydrogen bonding partners or bond strengths, so the initial OD-stretch frequency is highly correlated with the final. Given more time, this correlation vanishes, giving rise to rounder spectra. This loss of correlation is called spectral diffusion and is quantified by the FFCF. We see that spectral diffusion, and hence the decay of the FFCF, is slower for lower temperatures, a trend that extends into the supercooled region.

A series of different metrics have been proposed to qualitatively extract the FFCF from 2D IR spectra. Commonly used are the dynamic line width,<sup>33</sup> the nodal slope,<sup>34</sup> the line of constant phase,<sup>35</sup> or the center line of slope.<sup>36</sup> Here our metric of preference is the center line slope of the 0–1 lobe, shown as the green line in Figure 2. To acquire the value of the slope in a consistent way and hence to enable a comparison of the correlation decays for different temperatures, a linear fit is performed around the minimum (blue lobe, by convention), using for all population times and temperatures the same number of points.

The decay of the center line slope is shown in Figure 4 for temperatures (a) 260, (b) 265.5, (c) 273, and (d) 293 K measured at the magic angle. The curves are nonexponential because of multiple overlapping processes with different dynamics. Multiexponential fitting, however, proved to be inconsistent for different temperatures. So we perform a monoexponential fit of all data from 50 fs up to 2 ps, which we force to decay to zero. Beyond 2 ps, the population signal becomes very small (Figure 3) and might be affected by a background signal that is due to small residual scattering from the pump beam as well as an additional contribution from thermalization effects.<sup>23</sup> The fit performed in this way reveals that the correlation decay slows down from 710 fs for ambient conditions (293 K) to 2.6 ps for the supercooled regime (260 K). The absolute values of these decay constants depend to some extent on the metric of choice,<sup>35</sup> as well as to the fitting procedure (e.g., single or multiexponential, permitting an offset or not, fit up to 2 or 3 ps); however, we verified that the relative changes with temperature, that is, the slopes in Figure 5, are independent of the data treatment.

## DISCUSSION

One possible interpretation for the slower spectral diffusion rate at lower temperatures would be in the framework of an Arrhenius law:

$$\frac{1}{\tau_c} = A \exp\left(-\frac{E_a}{RT}\right) \quad (1)$$

The fit of the data (Figure 5a blue circles) reveals a slope of  $E_{a,\text{magic}} = 6.2 \pm 0.2$  kcal/mol, which would correspond to the value of the typical activation barriers that dominate water diffusion. The pre-exponential factor, in turn, comes out to be very fast with  $1/A = 0.02 \pm 0.01$  fs. Similar measurements

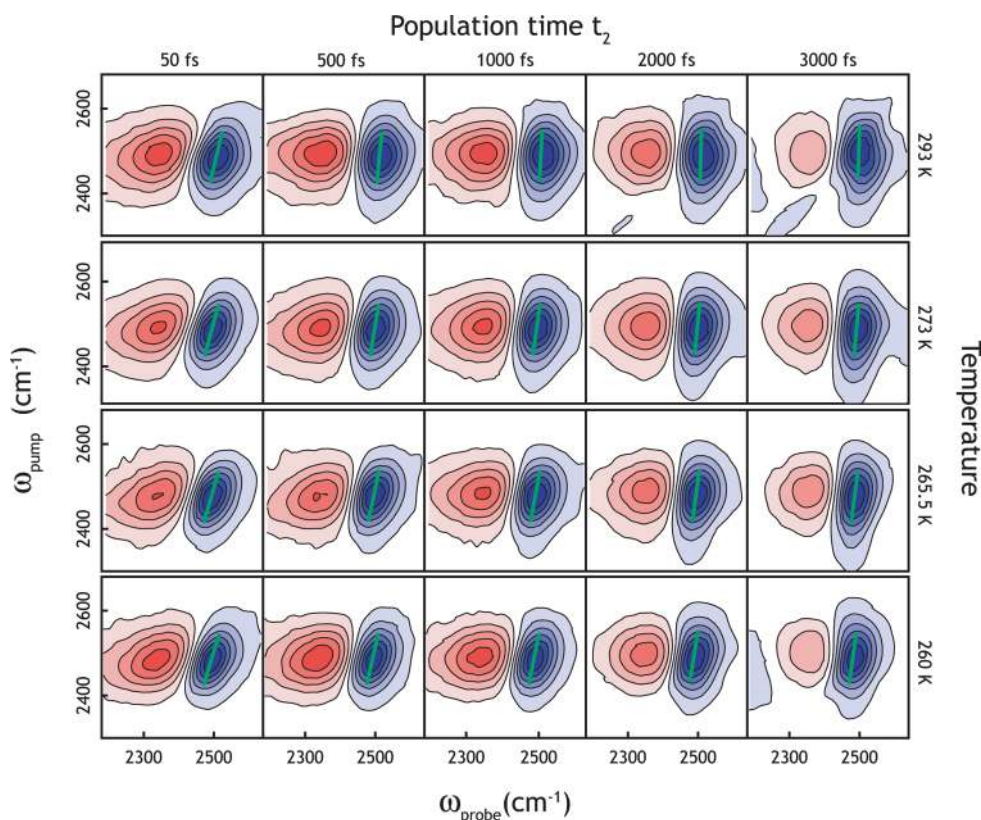


**Figure 2.** Purely absorptive 2D IR spectra of HOD in H<sub>2</sub>O for population times  $t_2 = 50, 500, 1000, 2000,$  and  $3000$  fs and for four different temperatures:  $T = 293, 273, 265.5,$  and  $260$  K, respectively. In green is the center line slope.

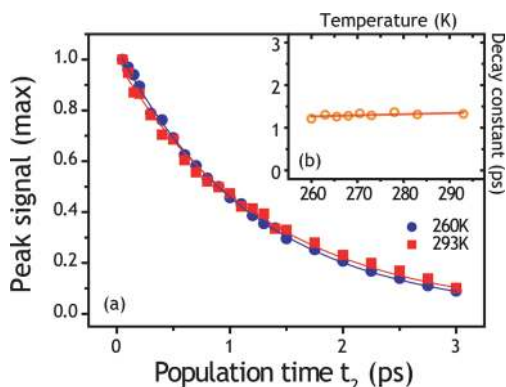


**Figure 3.** Vibrational relaxation, which does not exhibit a strong temperature dependence. (a) The peak signal decay for the two extreme temperatures (260 and 293 K). (b) The decay constants extracted by single exponential fit for different temperatures.

performed by Tokmakoff and co-workers for HOD/H<sub>2</sub>O at ambient temperatures, and in parallel polarization geometry  $\langle ZZZZ \rangle$  revealed an apparent barrier height of  $E_a = (3.4 \pm 0.5)$  kcal/mol,<sup>23</sup> nearly half of our value, and  $1/A = 2.0 \pm 1.0$  fs. To resolve this discrepancy, we repeated the measurements in parallel polarization and treated the data in exactly the same manner as before (data not shown). The result is the red squared points in Figure 5a. A linear fit reveals a barrier height of  $E_{a,par} = (3.5 \pm 0.2)$  kcal/mol, in perfect agreement with Tokmakoff and coworkers.<sup>23</sup> The difference between the measurements with the magic angle and parallel polarization originates from

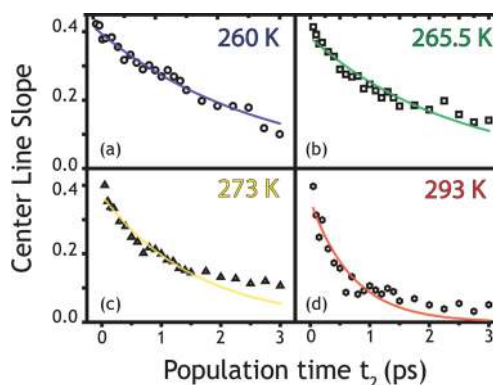


**Figure 4.** Decay of the center line slope with a single exponential fit, for temperatures: (a) 260, (b) 265.5, (c) 273, and (d) 293 K, measured at the magic angle.

the frequency-dependent anisotropy decay,<sup>27,28</sup> which changes the 2D IR line shape and hence affects the value of the metric used to extract spectral diffusion. Even though the frequency-dependent anisotropy decay evidence that the FFCF and the orientation correlation function do not decouple in a strict sense, we believe that the 2D IR response in the magic angle is the least affected by orientational relaxation.

The activation barrier in an Arrhenius scenario would be determined by the energy it costs to break a hydrogen bond before another one can be formed. A comparison of the deduced activation energy barrier (6.2 kcal/mol) with literature values for the strength of hydrogen bonds in water, obtained by simulations



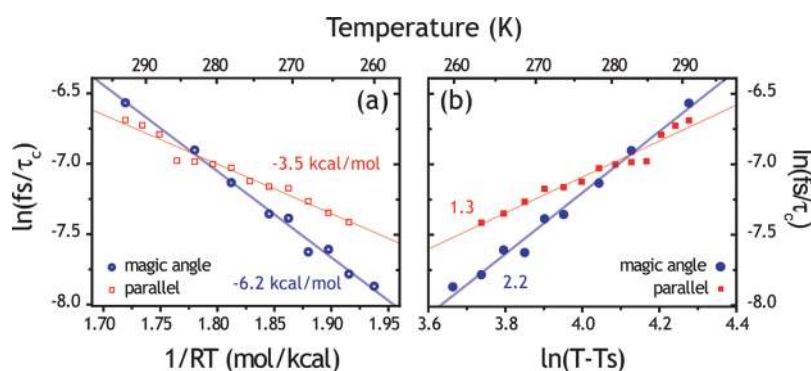


**Figure 5.** Decay constant  $\tau_c$  for different temperatures fitted with an Arrhenius law (a) and with a power law (b) for the magic angle (blue circles) and parallel geometry (red squares). In (a) the calculated barrier heights are shown next to the fits (kcal/mol), and in (b) the corresponding power law parameters  $\gamma$  are shown (see text).

(1.9 kcal/mol)<sup>37</sup> or experiments (1.5 kcal/mol),<sup>38</sup> leads to the conclusion that our value is tentatively too large. Furthermore, the pre-exponential factor of  $1/A = 0.02 \pm 0.01$  fs, which would be related to the inertial motion of water molecules (except when the activation barrier is strongly entropically favored), is unphysically fast.

An alternative interpretation is based on mode coupling theory,<sup>39</sup> typically used to describe supercooled liquids near the glass transition. In this context, heterodyned detected optical Kerr effect measurements (HD-OKE) performed by Righini and coworkers<sup>26</sup> in the supercooled regime were fitted to a power law to quantify the temperature dependence of the relaxation time scales (0.22 ps for 314 K up to 2.20 ps for 254 K). To examine the agreement with our results, we fit the data also to a power law of the type:

$$\tau_c = a(T - T_s)^{-\gamma} \quad (2)$$

where  $T_s$  is the singularity temperature. Near  $T_s$ , many dynamic quantities of water (such as viscosity and relaxation times) as well as thermodynamic ones (isothermal compressibility) seem to diverge.<sup>10</sup> Here for comparison we use the value obtained by Righini and coworkers<sup>26</sup> of  $T_s = 221$  K as a fixed parameter for fitting, since a free fit for all three parameters ( $a$ ,  $\gamma$ ,  $T_s$ ) did not converge. The result of the fit is shown in Figure 5b, where the power law parameter obtained for the magic angle data  $\gamma_{\text{magic}} = 2.2 \pm 0.1$  perfectly agrees with the HD-OKE result.<sup>26</sup> The HD-OKE experiment measures the orientational relaxation of water molecules, whereas the 2D IR experiment is sensitive to hydrogen-bond breaking and making, as well as the strength of these hydrogen bonds. As the same scaling laws are observed for both experiments, we conclude that both types of structural dynamics are correlated. In simple words, a water molecule can reorient only if it changes its hydrogen-bond partner.<sup>40</sup> The fit of the 2D IR data measured with parallel polarization (5b, red squares,  $\gamma_{\text{par}} = 1.3 \pm 0.1$ ), in contrast, deviates from Righini and coworkers,<sup>26</sup> providing further evidence that the magic angle measurements reflect better the underlying physical mechanism.

Both fits in Figure 5a and b are equally good, and we could not use the quality of the fits per se to decide whether  $\tau_c$  changes with temperature as a single barrier hopping process (Arrhenius) or as a multibarrier (power law) transition. This ambiguity is due to the small temperature range of this study which does not allow us to discriminate eq 1 from eq 2; a temperature much closer to  $T_s$  would be needed to safely make this distinction. Nevertheless, a fit within the framework of an Arrhenius law reveals unphysical

values for both the activation energy and the pre-exponential factor, so we tentatively conclude that the Arrhenius law is not the correct physical picture to describe the dynamics of supercooled water. In any case, our results are in very good agreement with measurements performed both in ambient conditions<sup>23</sup> as well as in the supercooled regime.<sup>26</sup> Considering this fact along with the actual tendency of our data, we conclude that the dynamical properties of water do not change in an abrupt manner as we enter the metastable supercooled regime, in contrast to the discontinuity observed when ice is formed.<sup>32</sup>

## CONCLUSIONS

In summary, we performed FTIR and 2D IR spectroscopy of isotopically substituted water from ambient temperature conditions (293 K) down to the supercooled regime (260 K). From the stationary measurements we observe red-shifting and narrowing of the OD stretch band as we lower temperature. This suggests the passage to a less inhomogeneous distribution of hydrogen-bonding environments (narrowing) which also appear to be more strongly hydrogen-bonded (red-shift). The 2D IR measurements allow us to quantify the temperature dependence of the decay of the FFCF, which provides information about the time scales of the hydrogen bonding system reorganization. This process takes longer for lower temperatures, suggesting that the interchange between the possible hydrogen-bonded configurations happens slower. As an Arrhenius fit of the temperature dependence of the correlation loss reveals unphysical parameters for both the barrier height and the pre-exponential factor, we tentatively conclude that it follows a power law with an exponent  $\gamma = 2.2$  and the singularity temperature  $T_s = 221$  K. As a side aspect of this work, we also show that measuring the 2D IR response in parallel polarization  $\langle ZZZZ \rangle$  can severely affect the results due to the coupling of spectral diffusion to the frequency-dependent anisotropy decay.

Recent 3D IR experiments of isotope-diluted water at ambient conditions reveal inhomogeneous structures with heterogeneous dynamics.<sup>5</sup> Surely, it would be interesting to see how the 3D IR response depends on temperature, especially down to the supercooled regime, which could possibly offer another viewpoint on the liquid–liquid phase transition debate.<sup>9</sup>

## AUTHOR INFORMATION

### Corresponding Author

\*E-mail: phamm@pci.uzh.ch.

## ACKNOWLEDGMENT

We would like to thank Dr. Jan Helbing and Julien Rehaalt for their precious contribution in the lab, as well as to Dr. Sean Garrett-Roe and Dr. Paul Donaldson for valuable discussions and comments. This work was supported by the Swiss National Science Foundation (SNF) through the NCCR MUST.

## REFERENCES

- (1) Debenedetti, P. G. *J. Phys.: Condens. Matter* **2003**, *15*, R1669–R1726.
- (2) Stillinger, F. H. *Science* **1980**, *209*, 451–457.
- (3) Tokushima, T.; Harada, Y.; Takahashi, O.; Senba, Y.; Ohashi, H.; Pettersson, L. G. M.; Nilsson, A.; Shin, S. *Chem. Phys. Lett.* **2008**, *460*, 387–400.
- (4) Huang, C.; Wikfeldt, K. T.; Tokushima, T.; Nordlund, D.; Harada, Y.; Bergmann, U.; Niebuhr, M.; Weiss, T. M.; Horikawa, Y.; Leetmaa, M.; et al. *Proc. Natl. Acad. Sci. U.S.A.* **2009**, *106*, 15214–15218.
- (5) Garrett-Roe, S.; Perakis, F.; Hamm, P. **2010**, *Proc. Natl. Acad. Sci. USA*, submitted.
- (6) Zasetsky, A. Y.; Khalizov, A. F.; Sloan, J. J. *J. Chem. Phys.* **2004**, *121*, 6941–6947.
- (7) Yada, H.; Nagai, M.; Tanaka, K. *Chem. Phys. Lett.* **2008**, *464*, 166–170.
- (8) Kim, K.; Saito, S. *J. Chem. Phys.* **2010**, *133*, No. 044511.
- (9) Mishima, O.; Stanley, H. E. *Nature* **1998**, *396*, 329–335.
- (10) Angell, C. A. *Annu. Rev. Phys. Chem.* **1983**, *34*, 593–630.
- (11) Lawrence, C. P.; Skinner, J. L. *J. Chem. Phys.* **2003**, *118*, 264–272.
- (12) Mukamel, S. *Principles of Nonlinear Optical Spectroscopy*; Oxford University Press: New York, 1995.
- (13) Hamm, P.; Zanni, M. T. *Concepts and Methods of 2D Infrared Spectroscopy*; Cambridge Press: Cambridge, U.K., 2011.
- (14) Cowan, M. L.; Bruner, B. D.; Huse, N.; Dwer, J. R.; Chung, B.; Nibbering, E. T.; Elsaesser, T.; Miller, R. J. D. *Nature* **2005**, *434*, 199–202.
- (15) Paarmann, A.; Hayashi, T.; Mukamel, T.; Miller, R. J. D. *J. Chem. Phys.* **2009**, *130*, 204110.
- (16) Steinel, T.; Asbury, J. B.; Zheng, J.; Fayer, M. D. *J. Phys. Chem. A* **2004**, *108*, 10957–10964.
- (17) Corcelli, S. A.; Lawrence, C. P.; Asbury, J. B.; Steinel, T.; Fayer, M. D.; Skinner, J. L. *J. Chem. Phys.* **2004**, *121*, 8897–8900.
- (18) Steinel, T.; Asbury, J. B.; Corcelli, S. A.; Lawrence, C. P.; Skinner, J. L.; Fayer, M. D. *Chem. Phys. Lett.* **2004**, *286*, 295–300.
- (19) Yeremenko, S.; Pshenichnikov, M.; Wiersma, D. A. *Chem. Phys. Lett.* **2003**, *369*, 107–113.
- (20) Fecko, C. J.; Eaves, J. D.; Loparo, J. J.; Tokmakoff, A.; Geissler, P. L. *Science* **2003**, *301*, 1698–1702.
- (21) Corcelli, S. A.; Skinner, J. L. *J. Phys. Chem. A* **2005**, *109*, 6154–6165.
- (22) Paesani, F.; Yoo, S.; Bakker, H. J.; Xantheas, S. S. *J. Phys. Chem. Lett.* **2010**, *1*, 2316–2321.
- (23) Nicodemus, R. A.; Ramasesha, K.; Roberts, S. T.; Tokmakoff, A. *J. Phys. Chem. Lett.* **2010**, *1*, 1068–1072.
- (24) Tielrooij, K. J.; Petersen, C.; Rezus, Y. L. A.; Bakker, H. J. *Chem. Phys. Lett.* **2009**, *471*, 71–74.
- (25) Schwarzer, D.; Lindner, J.; Vöhringer, P. *J. Phys. Chem. A* **2006**, *110*, 2858–2867.
- (26) Torre, R.; Bartolini, P.; Righini, R. *Nature* **2004**, *428*, 296–299.
- (27) Stirnenmann, G.; Laage, D. *J. Phys. Chem. Lett.* **2010**, *1*, 1511–1516.
- (28) Ramasesha, R. A.; Nicodemus, R. A.; Mandal, A.; Tokmakoff, A. In *Ultrafast Phenomena XVII*, Proceedings of the 17th International Conference on Ultrafast Phenomena, Snowmass, CO, USA, July 19–23, 2010; Springer-Verlag: New York, 2010.
- (29) Hamm, P.; Kaindl, R. A.; Stenger, J. *Opt. Lett.* **2000**, *25*, 1798–1800.
- (30) DeFlores, L. P.; Nicodemus, R. A.; Tokmakoff, A. *Opt. Lett.* **2007**, *32*, 2966–2968.
- (31) Helbing, J.; Hamm, P. **2010**, *J. Opt. Soc. Am. B*, in press.
- (32) Woutersen, S.; Emmerichs, U.; Nienhuys, H. K.; Bakker, H. J. *Phys. Rev. Lett.* **1998**, *81*, 1106–1109.
- (33) Asbury, J. B.; Steinel, T.; Stromberg, C.; Corcelli, S. A.; Lawrence, C. P.; Skinner, J. L.; Fayer, M. D. *J. Phys. Chem. A* **2004**, *108*, 1107–1119.
- (34) Demirdöven, N.; Khalil, M.; Tokmakoff, A. *Phys. Rev. Lett.* **2002**, *89*, 237401.
- (35) Roberts, S. T.; Loparo, J. J.; Tokmakoff, A. *J. Chem. Phys.* **2006**, *125*, No. 084502.
- (36) Bakulin, A. A.; Liang, C.; Jansen, T. L.; Wiersma, D. A.; Bakker, H. J.; Pshenichnikov, M. S. *Acc. Chem. Res.* **2009**, *42*, 1229–1238.
- (37) Silverstein, K. A. T.; Haymet, A. D. J.; Dill, K. A. *J. Am. Chem. Soc.* **2000**, *122*, 8037–8041.
- (38) Smith, J. D.; Cappa, C. D.; Wilson, K. R.; Messer, B. M.; Cohen, R. C.; Saykally, R. J. *Science* **2004**, *306*, 851–853.
- (39) Fabian, L.; Latz, A.; Schilling, R.; Sciortino, F.; Tartaglia, P.; Theis, C. *Phys. Rev. E* **1999**, *60*, 5768–5776.
- (40) Laage, D.; Hynes, J. T. *Science* **2006**, *311*, 832–835.